Int. J. Electrochem. Sci., 17 **(2022)** Article Number: 22128, doi: 10.20964/2022.12.11

International Journal of
ELECTROCHEMICAL
SCIENCE
www.electrochemsci.org

Short Communication

A Low Cost, High Electrochemical Performance Carbon Coated Zinc Borate Anode Material for Sodium-ion Batteries

Mengqi Jiang [1], Yongjie Cao [2,], Yao Liu [2], Ruiqi Wang [1], Tong Chen [3,*], Junxi Zhang [1,*]*

[1] Shanghai Key Laboratory of Materials Protection and Advanced Materials in Electric Power, Shanghai University of Electric Power, Shanghai, 200090, P. R. China
[2] Department of Chemistry and Shanghai Key Laboratory of Molecular Catalysis and Innovative Materials, Fudan University, Shanghai 200433, P. R. China.
[3] Huadian Electric Power Research Institute, Hangzhou, China
[*]E-mail: tcheng0821@163.com

Received: 21 August 2022 / *Accepted:* 27 October 2022 / *Published:* 17 November 2022

Sodium-ion batteries (SIBs) as an ideal candidate for large-scale energy storage have been widely studied due to the low cost and almost unlimited sodium resource on the earth, but the works on exploring the high electrochemical performance anode materials with low-cost and eco-friendly are still urgently needed. Herein, with the assistance of a simple liquid co-precipitation method and subsequent chemical vapor deposition (CVD) treatment, the environmentally friendly, low cost and nontoxic $Zn_3(BO_3)_2$@C (ZBO@C) composite is directly synthesized and proves to be an ideal anode material for SIBs. As anode material, it demonstrates a high initial reversible discharge specific capacity of 289.8 mAh g^{-1} with a corresponding Coulombic efficiency of 53.7 % at 0.03 A g^{-1}. Even at 1 A g^{-1}, it still exhibits a reversible specific capacity of 151 mAh g^{-1} after 500th cycles with almost no capacity losing. The Na-ion full cell (ZBO@C||NaCuFeMnO) exhibits a maximum energy/power density of 119 Wh kg^{-1}/301 W kg^{-1} based on the total mass loading of anode and cathode. Those results indicate that the ZBO@C is an ideal anode for future large-scale energy storage.

Keywords: Energy storage; Sodium-ion batteries; Anode material; Zinc borate

1. INTRODUCTION

The increasing natural resources scarcities and environmental pollution have received the human's continuous attention to develop and utilize the renewable energy such as solar energy, wind energy or tidal energy [1-3]. Meanwhile, sodium-ion batteries (SIBs) possess a huge application prospect in large-scale energy storage (LSES), which are considered as outstanding energy storage devices for renewable energy due to its' low cost and almost unlimited sodium sources on the earth [4-7]. However, the major problem in realizing the practical application of SIBs lies in the development of the high

electrochemical performance electrode materials, especially low-cost anode materials [8-10]. Up to now, considering on the cost and environmental protection factors, the main type of anode materials for SIBs are hard/soft carbon and low-cost transitional metal (Mn, Fe) oxides [8-13]. But some drawbacks of these materials are noticeable; for instance, the main capacity of hard carbon exhibits at a potential (0.1 V) that closes to Na metal plating which results in Na dendrite formation and causes a safe hidden trouble [8-10]. The low temperature treated soft carbon as anode possesses an inclined platform with high safety, but the reversible specific capacity is less than 260 mAh g^{-1}, which has obviously limited the energy density in SIBs [11]. The transitional metal (Mn, Fe) oxides such as Co_3O_4 and Fe_2O_3 as anodes in SIBs show high theoretical capacity, but the large volume and particle pulverization effect have seriously affected its' cycle life [12, 13].

Inorganic borates as electrode materials have been widely developed and researched in the past decades due to its low cost and stable BO_3^- triangle polyanion-type structure. The borate materials are considered as an ideal candidates anode materials for Li or Na-ion batteries since 1997, and some following researchers are focused on Fe_3BO_5, $Cu_3B_2O_6$, $Ni_3(BO_3)_2$, $Co_3B_2O_6$, however this kinds of anode materials exhibit much inferior electrochemical performance when compare with its' corresponding oxide materials [14-17]; Considering of the cost and environmental factors, the nontoxicity and environmental friendliness of $Zn_3(BO_3)_2$ (donated ZBO) anode material, which is very meaningful and interesting to research the developing green and facile synthesis method for improving the Na-ion storage abilities.

In this work, an ultra-thin carbon coated ZBO (donated ZBO@C) composite is green chemically synthesized through a simple liquid phase coprecipitation combining with CVD method. As anode material in SIBs, the ZBO@C shows a high reversible discharge capacity of 289.8 mAh g^{-1} at 0.03 A g^{-1}, even at 1 A g^{-1}, it still exhibits a reversible discharge capacity of 147.4 mAh g^{-1} and retains capacity of 151 mAh g^{-1} after 500th cycles. The Na-ion full cell (ZBO@C||NaCuFeMnO) shows a maximum energy/power density of 119 Wh kg^{-1}/301 W kg^{-1} basing on the total mass loading of both anode and cathode. These results show that the ZBO@C as anode materials in SIBs possess low-cost and high electrochemical performance, which is an ideal anode material for LSES in the future.

2. EXPERIMENTAL SECTION

2.1. Materials Preparation

The zinc borate (ZBO) was synthesized via a simple liquid co-precipitation method. First, the 0.03 mol $Zn(NO_3)_2$•$6H_2O$ was dissolved in 80 mL of deionized water and heated to 70 °C. Then slowly added 0.01 mol $Na_4B_4O_7$•$10H_2O$ (dissolved in 20 mL deionized water) via a quickly magnetic stirring for 2 h. The prepared precursor-precipitate was washed several times using hot deionized water (70 °C). The washed-precursor was dried in an oven at 120 °C for 12 h, and following heated at 700 °C for 2 h in a tube furnace in Air atmosphere. Finally, a white color power of ZBO was synthesized. The carbon coated ZBO was prepared by a chemical vapor deposition method (CVD) through using the obtained ZBO power heated in N_2 atmosphere at 700 °C for 2 h under a heating rate of 3 °C/min. The carbon

source was a toluene gas with a flow rate at 20 mL min^{-1}. All of the reagents used are analytically pure (AR) without any further treatment.

2.2. Characterization

The crystal information was tested via a powder X-ray diffraction (XRD, Bruker D8, Germany) with a *Cu Kα* radiation X-ray diffractometer (λ = 0.1546 nm), and the scanning speed was 0.1° min^{-1} in a range from 10 to 80°. The morphology and microstructure were investigated via a field emission scanning electron microscopy (SEM, JSM-7800F, Japan) and a high-resolution transmission electron microscopy (HR-TEM, JEM-2100F, Japan).

2.3. Electrochemical Test

All of the electrochemical experiments were tested under room temperature (25℃).

All of electrochemical tests were conducted in the CR-2016 type coin cells. The ZBO and ZBO@C anode were obtained by using the weight ratio of active material, conductive agent (super P) and binder in 8:1:1. The binder was carboxyl methylcellulose (CMC). After mixed for 4 h via a planetary ball mill for 4 h, the slurry was uniformly coated on the copper foil. After dried in an oven for 12 h at 120 ℃, the prepared-electrode was cut into 14 mm disk in an average mass loading of 3-4 mg cm^{-2}. The coin-cell was assembled via a sodium tablets as counter electrode, a Whatman glass fiber as the separator, and the electrolyte was used the 1 M $NaPF_6$ in ethylene carbonate (EC, AR, Sinopharm), Ethyl Methyl Carbonate (EMC, AR, Sinopharm), and 5 vol.% fluoroethylene carbonate (FEC) as the additive. The charge/discharge process were tested via a Wuhan Land CT2001A battery system.

3. RESULTS AND DISCUSSION

The XRD results of ZBO and ZBO@C were shown in Figure 1 (a), which could be indexed to the pure phase structure of ZBO (PDF: 37-1486) without any crystalline impurity. The crystal structure of ZBO was shown in Figure 1 b, which indicated that it was a typical monoclinic structure built by the BO_3-triangle sharing common vertices with the ZnO_4-tetrahedra corresponding to lattice cell parameters of a= 2.34 Å, b= 5.04 Å, c= 8.38 Å, V= 99.25 $Å^3$ [18-20].

The morphology and microstructure of ZBO@C were shown in Figure 2. As shown in Figure 2 (a, b), the ZBO@C showed a spherical shape with an average primary particle size ranged from 50-100 nm. The TEM images illustrated in Figure 2 (c, d), which could see that the ZBO@C spherical particle exhibited a typical core shell structure with a uniform carbon layer (3-5 nm) on the surface of ZBO. The HR-TEM image showed in Figure 2 (e) indicated that an ultrathin carbon (3 nm) coated on the surface of ZBO, and the crystal plane of (021) and (200) showed the corresponding lattice spacing of 1.3 and 2.6 Å, respectively. The selected area electron diffraction pattern (SAED) indicated that the ZBO@C showed a well crystallinity, which was consistent with the XRD result (Figure 1 a).

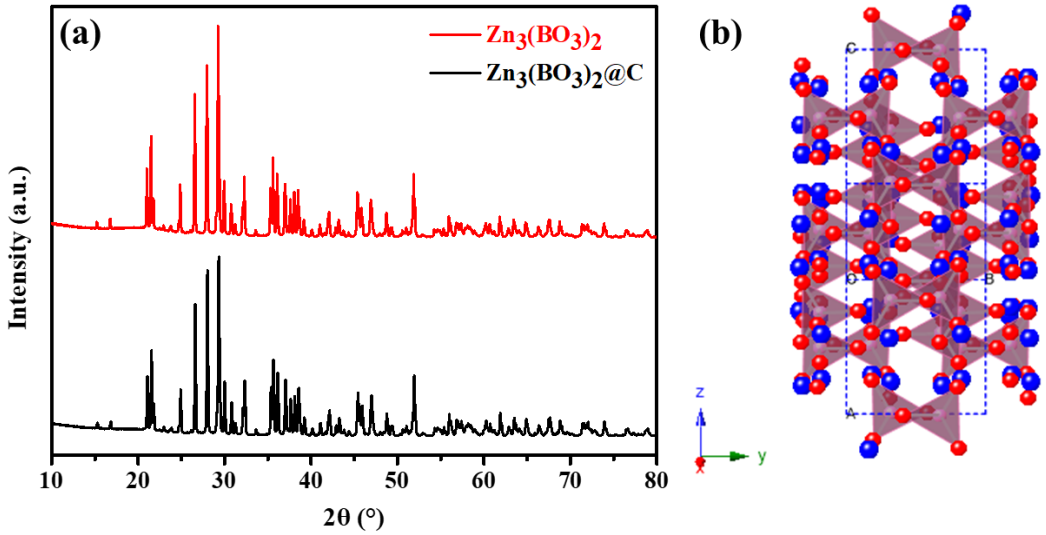

Figure 1. (a) The XRD pattern of ZBO and ZBO@C; **(b)** The crystallographic structure of ZBO.

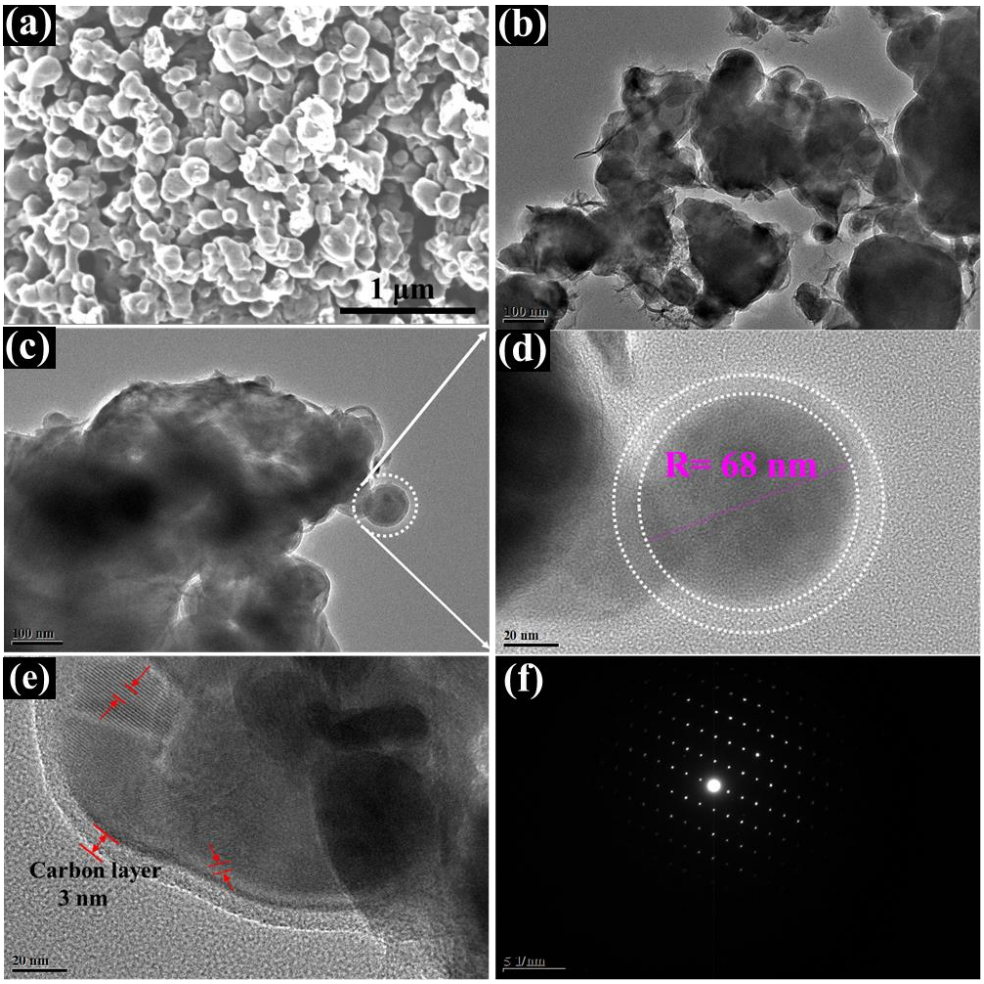

Figure 2. (a) SEM image of ZBO@C; **(b-d)** TEM images of ZBO@C; **(e)** HR-TEM image of ZBO@C; **(f)** Selected area electron diffraction pattern.

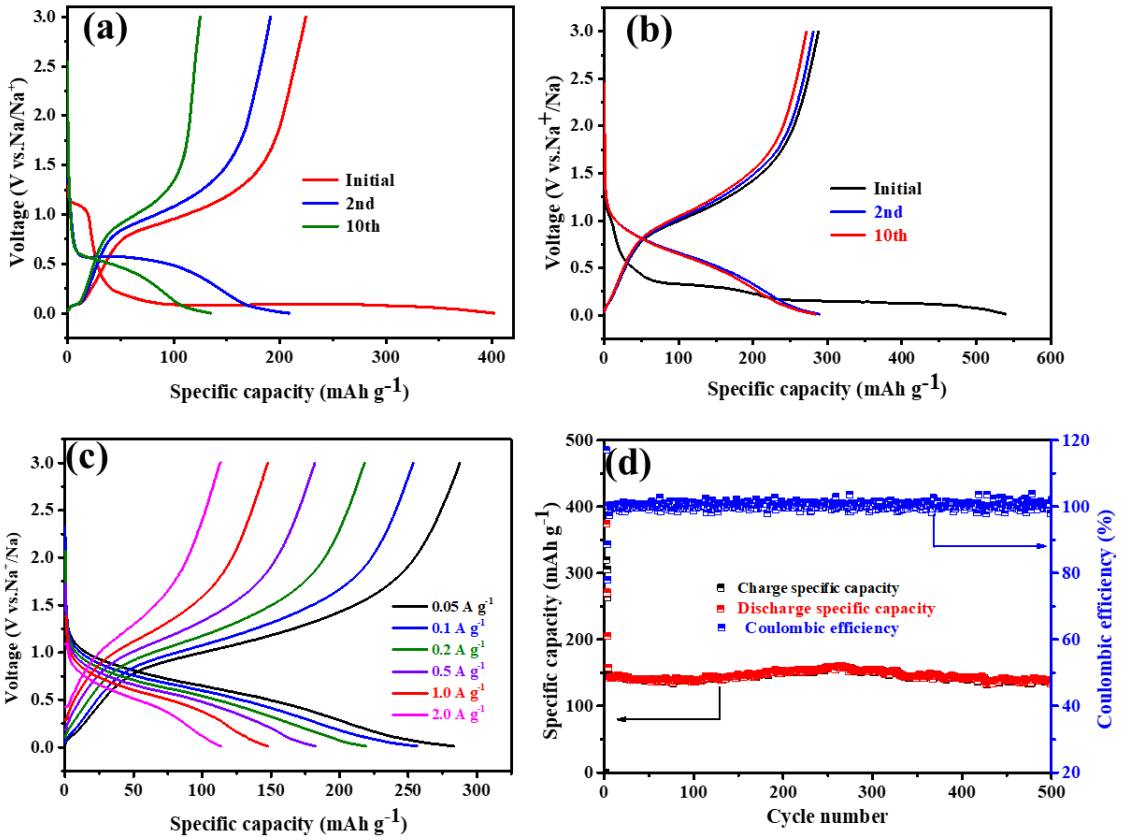

Figure 3. (a) The 1st-10th charge/discharge curves of ZBO at 0.1 C in SIBs; **(b)** The 1st-10th charge/discharge curves of ZBO@C at 0.1 C in SIBs; **(c)** The rate capabilities of ZBO@C in SIBs; **(d)** The cycle stability of ZBO@C at 1 A g^{-1}.

The electrochemical performance of the sodium-ion half-cell was shown in Figure 3. As comparison, the sodium-ion storage performance of ZBO and ZBO@C anode were shown in Figure 3 (a, b), which we could see that the ZBO anode material showed an initial discharge specific capacity of 224.5 mAh g^{-1} with a corresponding Coulombic efficiency of 55.8% and just maintained at 55.7 % specific capacity after 10th cycles at 0. 1 C (1 C = 300 mA g^{-1}) in SIBs. On the other hand, the ZBO@C anode material showed an initial discharge specific capacity of 539.7 mAh g^{-1} with a corresponding Coulombic efficiency of 53.7 % and keep a discharge capacity retention of 93.9 % after 10th cycles at 0.1 C in SIBs. The rate capabilities of ZBO@C anode in SIBs (Figure 3 (c)) showed a reversible discharge specific capacity of 287.6, 256.5, 219.7, 182.4, 147.4 and 113.5 mAh g^{-1} at 0.05, 0.1, 0.2, 0.5, 1.0 and 2.0 A g^{-1}, respectively. The cycle-stability of ZBO@C anode was showed in Figure 3 (d), which indicated that it exhibited a reversible specific capacity of 151 mAh g^{-1} with almost no capacity losing at 1.0 A g^{-1} after 500th cycles in SIBs. The cycle performance of various anode materials in sodium-ion batteries were shown in Table 1, which indicated that the nanotechnology combining with CVD carbon coating method could effectively improve the cycle stability of anode materials.

The sodium-ion full cell was matched using the ZBO@C as anode and layered metal oxide $Na_{0.9}[Cu_{0.22}Fe_{0.30}Mn_{0.48}]O_2$ (donated NaCuFeMnO) [21] as cathode. As shown in Figure 4 (a), the sodium-ion full cell (ZBO@C||NaCuFeMnO) exhibited a reversible discharge specific capacity of 267.3

mAh g^{-1} (based on the anode mass loading) and maintained at 75 % specific capacity after 10th cycles at 0.1 C. The rate capability of ZBO@C||NaCuFeMnO sodium-ion full cell was shown in Figure 4 (b, c), which showed a reversible specific capacity of 267.3, 230.6, 202.2, 174.5, 155.2 and 135.7 mAh g^{-1} at 0.1, 0.2, 0.5, 1.0, 2.0 and 5.0 C, respectively. The energy/power density of ZBO@C||NaCuFeMnO full cell was shown in Figure 4 (d), which indicated that it showed a maximum energy/power density of 119 Wh kg^{-1}/301 W kg^{-1} based on the total mass loading of both anode and cathode.

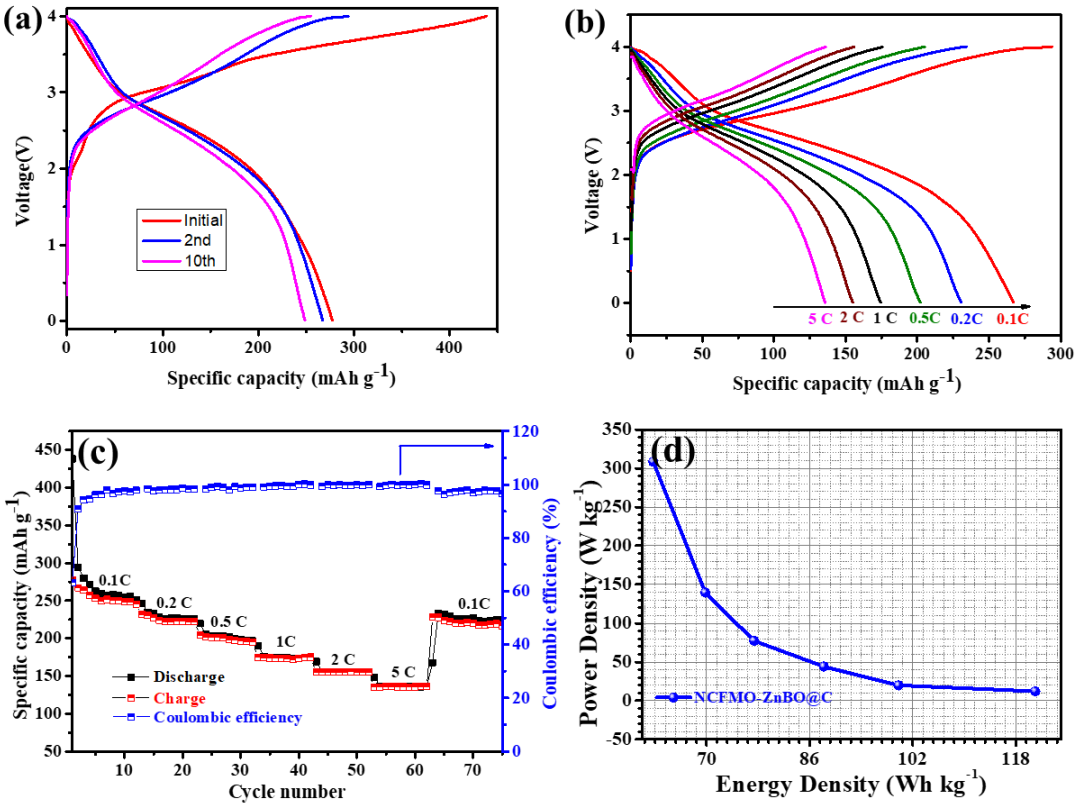

Figure 4. (a) The 1st-10th charge/discharge curve of ZBO@C||NaCuFeMnO sodium-ion full cell at 0.1 C; **(b**, **c)** The rate capability of ZBO@C||NaCuFeMnO sodium-ion full cell; **(d)** The energy/power density of ZBO@C||NaCuFeMnO sodium-ion full cell.

Table 1. The cycle performance of various anode materials in sodium-ion batteries.

Cathode material	Voltage window (V)	Cycle performance	References
Fe_3BO_5	0.01-3.0	380 mAh g^{-1} at 0.4 A g^{-1} after 100cycles	(15)
$Ni_2(BO_3)_3$	0.01-3.0	425 mAh g^{-1} at 0.1 A g^{-1} after 50 cycles	(16)
$Zn_3(BO_3)_2$@NC	0.01-3.0	270 mAh g^{-1} at 0.1 A g-1 after 30 cycle	(20)
$FeBO_3$	0.01-3.0	382 mAh g^{-1} at 0.4 A g^{-1} after 100 cycles	(22)

$Co_2B_2O_5$	0.01-3.0	324 mAh g^{-1} at 0.1 A g^{-1} after 60 cycles	(23)
TiO_2	0.01-2.5	177 mAh g^{-1} at 0.4 A g^{-1} after 150 cycles	(24)
$FeVBO_4$	0.01-2.5	46 mAh g^{-1} at 0.01 A g^{-1}	(25)
Ce-V_5S_8	0.01-3.0	109 mAh g^{-1} at 1.0 A g^{-1} after 100 cycles	(26)
1T-MoS2	0.01-3.0	300 mAh g^{-1} at 1 A g^{-1} after 350 cycles	(27)
$Zn_3(BO_3)_2$@C	0.01-3.0	151 mAh g^{-1} at 1 A g^{-1} after 500 cycles	This work

4. CONCLUSION

In summary, an ultrathin carbon-coated ZBO anode materials has been synthesized. The sodium-ion storage performance is outstanding such as in cycling stability and rate capability. The sodium-ion full cell using NaCuFeMnO cathode and ZBO@C anode showed a reversible discharge specific capacity of 267.3 mAh g^{-1} and maintains at 75 % specific capacity after 10^{th} cycles at 0.1 C. And the full cell possesses an average voltage of 2.5 V with a maximum energy/power density of 119 Wh kg^{-1}/301 W kg^{-1} based on the total mass loading of both anode and cathode. These results showed that the ZBO@C as anode materials in SIBs possessed low-cost and high electrochemical performance, which was an ideal anode material for LSES in the future in the future.

ACKNOWLEDGEMENTS
This work was financially supported by Science and Technology Commission of Shanghai Municipality (19DZ2271100).

References

1. P. K. Nayak, W. F. Brehm and P. Adelhelm, *Angew. Chem. Int. Ed*., 57 (2018**)**, 102-120.
2. X. Y. Zheng, W. Luo, L. H. Jiang, Y. N. Hao, Y. H. Huang, *Energy. Storage. Mater*., 16 (2019) 6-23.
3. T. F. Liu, Z. G. Jiang, X. Q. Zeng, J. P. Ji, Z. H. Li, X. H. Gao, M. H. Sun, Z. Lin, J. C. Zheng and C. D. Liang, *Energy. Environ. Sci.,* 12 (2019) 1512-1533.
4. J. Ding, E. S. Peak and D. Mitlin, *Chem. Rev*., 118 (2018**)** 6457-6498.
5. H. L. Pan, Y. S. Hu and L. Q. Chen, *Energy. Environ. Sci*., 6 (2013) 2338-2360.
6. J. Zhao, F. X. Wang, C. Wang, S. Wang, C. Y. Wang, Z. W. Zhao, L. L. Duan, Y. P. Liu, Y. P. Wu, W. Li, D. Y. Zhao, *Nano Energy*, 56 (2019) 426–433.
7. Y. Liu, J. X. Zhang, Y. Y. Xia, T. Chen and S. M. Zhang, *ACS Sustainable. Chem*. Eng., 5 (2017) 1306-1314.
8. Q. S. Meng, Y. X. Lu, F. X. Ding, Q. Q. Zhang, L.Q. Chen, Y. S. Hu, *ACS Energy Lett*., 4 (2019) 2608-2612.
9. X. Zhang, X. L. Dong, X. Qiu, Y. J. Cao, C. X. Wang, Y. G. Wang, Y. Y. Xia, *J. Power Sources*, 476 (2020) 228550.

10. H. Au, H. Alptekin, A. C. S. Jensen, E. Olsson, C. A. O'Keefe, T. Smith, M. C. Ribadeneyra, T. F. Headen, C. P. Grey, Q. Cai, A. J. Drewb, M. M. Titiric, *Energy Environ. Sci*., 13 (2020) 3469.
11. Y. R. Qi, Y. X. Lu, F. X. Ding, Q. Q. Zhang, H. Li, X. J. Huang, Li. Q. Chen, Y. S. Hu, *Angew. Chem. Int. Ed*., 58 (2019) 4361-4365.
12. Y. J. Zhao, F. X. Wang, C. Wang, S. Wang, C. Y. Wang, Z. W. Zhao, L. L. Duan, Y. P. Liu, Y. P. Wu, W. Li, D. Y. Zhao, *Nano Energy*, 56 (2019) 426–433.
13. B. Y. Sun, S. F. Lou, W. Zheng, Z. Y. Qian, C. Cui, P. J. Zuo, C. Y. Du, J. Y. Xie, J. J. Wang, G. P. Yin, *Nano Energy*, 78 (2020) 105366.
14. Y. Y. Cao, X. L. Cao, X. L. Dong, X. Zhang, J. Xu, N. Wang, Y. Yang, C. X. Wang, Y. Liu, Y. Y. Xia, *Adv. Funct. Mater*., 31 (2021) 2102856.
15. Q. S. Ping, B. B. Xu, X. Ma, J. L. Y. Tian, B. F. Wang, *Dalton Trans*., 48 (2019) 5741.
16. B. B. Xu, Y. Liu, J. L. Y. Tian, X. Ma, Q. S. Ping, B. F. Wang, Y. Y. Xia, *Chem. Eng. J.,* 363 (2019) 285–291.
17. A. D. Bart, B. Revel, L. Dupont, L. Montagne, J. B. Leriche, M. Touboul, and J. M. Tarascon, *Chem. Mater*., 15 (2003) 3683-3691.
18. G. V. S. S. Sarma, C. V, Reddy, S. V. P. Venkat, C. R. Krishna, P. N. Murthy, R. V. S. S. N. Ravikumar, *J. Mol, Struct*., 1048 (2013) 64–68.
19. C. V. Reddy, G. V. S. S. Sarma, R. V. S. S. N. Ravikumar, J. Shim, C. V. P. Vattikuti, *Optik,* 127 (2016) 4536–4540.
20. S. Wang and X. B. Zhang, *Adv. Mater.,* 31 (2018) 1805432.
21. L. Q. Mu, S. Y. Xu, Y. M. Li, Y. S. Hu, H. Li, L. Q. Chen and X. J. Huang, *Adv. Mater*., 43 (2015) 6928-6933.
22. B. Z. Wu, S. Qi, X. K. Wu, H. L. Wang, Q. Q. Zhuang, H. M. Yi, P. Xu, Z. N. Xiong, G. J. Shi, S. Q. Chen, B. F. Wang, *Chinese Chem. Lett.,* 32 (2021) 3113-3117.
23. H. Chen, B. B. Xu, Q. S. Ping, B. Z. Wu, X. K. Wu, Q. Q. Zhuang, H. L. Wang, B. F. Wang, *Rare Metals*, 39 (2020) 1045–1052.
24. Z. X. Guan, K. X. Zou, X. Wang, Y. F. Deng, G. H. Chen, *Chinese Chem. Lett.*, 32 (2021) 3847-3851.
25. M. L. Dong, Q. Kuang, X. X. Zeng, L. Chen, J. Z. Zhu, Q. H. Fan, Y. Z. Deng, Y. M. Zhao, *J. Alloy. Compd.*, 812 (2020) 152165.
26. C. H. Yang, X. Ou, X. H. Xiong, F. H. Zheng, R. Z. Hu, Y. Chen, M. L. Liu and K. Huang, *Energy Environ. Sci.*, 10 (2017) 107-113.
27. C. Lane, D. X. Cao, H. Y. Li, Y. C. Jiao, B. Barbiellini, A. Bansil, and H. L. Zhu, *Condens. Matter.*, 4 (2019) 53.